GREEN BANK TELESCOPE STUDIES OF GIANT PULSES FROM MILLISECOND PULSARS

H. S. KNIGHT[1] AND M. BAILES

Centre for Astrophysics and Supercomputing, Swinburne University of Technology, P.O. Box 218, Hawthorn VIC 3122, Australia;
hknight@astro.swin.edu.au

R. N. MANCHESTER

Australia Telescope National Facility, CSIRO, P.O. Box 76, Epping NSW 1710, Australia

S. M. ORD[2]

Centre for Astrophysics and Supercomputing, Swinburne University of Technology, P.O. Box 218, Hawthorn VIC 3122, Australia

AND

B. A. JACOBY[3]

Department of Astronomy, California Institute of Technology, MS 105-24, Pasadena, CA 91125

Received 2005 August 29; accepted 2005 December 6

ABSTRACT

We have conducted a search for giant pulses from four millisecond pulsars using the 100 m Green Bank Telescope. Coherently dedispersed time series from PSR J0218+4232 were found to contain giant pulses of very short intrinsic duration whose energies follow power-law statistics. The giant pulses are in phase with the two minima of the radio integrated pulse profile but are phase-aligned with the peaks of the X-ray profile. Historically, individual pulses more than 10–20 times the mean pulse energy have been deemed to be "giant pulses." As only 4 of the 155 pulses had energies greater than 10 times the mean pulse energy, we argue the emission mechanism responsible for giant pulses should instead be defined through: (1) intrinsic timescales of microsecond or nanosecond duration; (2) power-law energy statistics; and (3) emission occurring in narrow phase windows coincident with the phase windows of nonthermal X-ray emission. Four short-duration pulses with giant-pulse characteristics were also observed from PSR B1957+20. As the inferred magnetic fields at the light cylinders of the millisecond pulsars that emit giant pulses are all very high, this parameter has previously been considered to be an indicator of giant-pulse emissivity. However, the frequency of giant-pulse emission from PSR B1957+20 is significantly lower than for other millisecond pulsars that have similar magnetic fields at their light cylinders. This suggests that the inferred magnetic field at the light cylinder is a poor indicator of the rate of emission of giant pulses.

Subject headings: pulsars: general — pulsars: individual (PSR J0218+4232, PSR J1012+5307,
PSR J1843−1113, PSR B1957+20)

1. INTRODUCTION

The Crab radio pulsar was discovered through the direct detection of strong individual pulses (Staelin & Reifenstein 1968). Further studies revealed that the strongest pulses followed power-law energy statistics (Argyle & Gower 1972) distinct from the Gaussian statistics of the general pulse population (Cordes 1976). In an observation by Lundgren et al. (1995), around 1 in 1200 pulses had an energy greater than 20 times the mean pulse energy, $\langle E \rangle$. Despite this, Cordes et al. (2004) found that at all radio frequencies phase-coherent summation of the giant pulses gives a higher signal-to-noise ratio than summation of all the pulses. Extraordinarily, the giant pulses also have structure that is significantly narrower than the mean pulse. Hankins et al. (2003) observed pulses that had structure persisting for less than 2 ns and inferred that the brightness temperatures of these pulses are $T_B \sim 10^{37}$ K.

The young Crab-like pulsar B0540−69 in the Large Magellanic Cloud also emits giant pulses (Johnston & Romani 2003). In 31.2 hr of observations at a center frequency of 1390 MHz, Johnston et al. (2004) only detected the integrated emission profile of PSR B0540−69 at a very low level of significance. Despite their difficulty in detecting the integrated emission, Johnston et al. were able to detect and analyze 141 individual pulses. The relative ease with which giant pulses can be seen over large distances has led several authors to advocate their detection as a way to find extragalactic pulsars (see, e.g., Johnston & Romani 2003; Cordes et al. 2004).

To date, no other young pulsars have been found to emit pulses with the high energies and extremely short durations characteristic of the giant pulses from the Crab pulsar. Three young pulsars have been found to emit narrow pulses of emission showing power-law statistics (Johnston et al. 2001; Johnston & Romani 2002; Cairns et al. 2004). However, it is not clear that the pulses should be classed as true "giant pulses," because the power-law tails have only been seen to extend to low energies. In addition, the structure of these events has thus far not been shown to have timescales as short as those of giant pulses from the Crab pulsar.

The recycled pulsars B1937+21, B1821−24, and J1823−3021A also emit giant pulses despite having periods (P) and period derivatives ($\dot{P}$) markedly different from those of the Crab pulsar (Cognard et al. 1996; Romani & Johnston 2001; Knight et al. 2005). One common factor between these millisecond pulsars, PSR B0540−69, and the Crab pulsar is that they all have very high magnetic fields inferred at their light cylinders,[4]

---

[4] The ATNF Pulsar Catalogue has been used to obtain the pulsar parameters and statistics used in this paper. See http://www.atnf.csiro.au/research/pulsar/psrcat.

TABLE 1
SUMMARY OF SEARCHES FOR GIANT-PULSE EMISSION

PSR (1)	ν (MHz) (2)	$\delta\nu$ (MHz) (3)	t_{obs} (s) (4)	N_p ($\times 10^5$) (5)	$\langle E \rangle$ (Jy μs) (6)	E_{lim} ($\langle E \rangle$) (7)	N_{det} (8)	Notes (9)
J0218+4232	857	128	3456	15	18	0.58	24, 75	1
	857	128	5216	22	9.2	0.95	5, 35	2
	1373	64	3349	14	3.9	2.5	4, 8	
	825	64	293	1.3	8.7	1.7	0, 4	
J1012+5307	825	64	720	1.4	60	0.27	0	
	1373	64	6077	12	15	0.72	0	
	1437	64	6951	13	22	0.51	0	
J1843−1113	825	64	3198	17	6.2	4.3	0	
	1373	64	791	4.3	2.3	5.8	0	
	1437	64	1436	7.8	1.9	6.9	0	
B1957+20	825	64	8003	50	4.7	4.0	4	
	1373	64	4684	29	0.72	16	0	3
	1437	64	4760	30	0.63	19	0	3

NOTES.—(1) 2004 August observation; (2) 2004 October observation; (3) No phase-coherent timing solution was available because of incorrect time tagging. The flux density (S) used to derive the given parameters is given by the $S = 0.35(\nu/1490\ \text{MHz})^{-3}$ mJy relation of Fruchter et al. (1990).

$B_{LC} \propto P^{-2.5}\dot{P}^{0.5}$. When viewed in the context of the known millisecond pulsar population, the three giant pulse emitters also have very low characteristic ages, $\tau = P/(2\dot{P})$, and very high spin-down luminosities, $\dot{E} \propto P^{-3}\dot{P}$. PSRs B1821−24, B1937+21, and J0218+4232 have some of the highest X-ray luminosities of all millisecond pulsars (Becker & Trümper 1999; Grindlay et al. 2002; Cusumano 2004; Heinke et al. 2005). The emission from all three pulsars is nonthermal, and the X-ray profiles of PSRs B1821−24 and B1937+21 align in phase with their giant pulse emission (Romani & Johnston 2001; Cusumano et al. 2003). Another field pulsar with a high X-ray luminosity is PSR B1957+ 20 (Becker & Trümper 1999). However, no X-ray pulsations have been detected from this source, and it is unclear how much of the emission originates from the bow shock between the pulsar wind and the companion wind (Stappers et al. 2003).

In this paper we present the results of a sensitive baseband search for microsecond-timescale emission from four millisecond pulsars. Upper limits are placed on emission from PSRs J1843−1113 and J1012+5307, and a new population of short-duration pulses is reported for PSR B1957+20. A previously unknown population of giant pulses from PSR J0218+4232 is characterized, and the results are used to clarify the defining characteristics of giant-pulse phenomenology.

2. OBSERVATIONS AND DATA ANALYSIS

All observations were taken using the 100 m NRAO Green Bank Telescope (GBT) from 2004 August to 2005 January at frequencies in the ranges of 793–921 and 1341–1469 MHz. Data were acquired using the Caltech–Green Bank–Swinburne Recorder II (see Jacoby 2005). This instrument real-samples one or two dual polarization 64 MHz wide bands at the Nyquist rate. Software algorithms similar to those described by van Straten (2003) were used to synthesize filter banks. The first step of the technique is to Fourier transform the raw voltages to the frequency domain and divide the spectra into a series of subbands. Each subband is multiplied by an inverse-response filter (kernel) for the interstellar medium (ISM; see, e.g., Hankins & Rickett 1975; Stairs 1998). The subbands are then individually Fourier transformed back to the time domain to give numerous time series, each having coarser time resolution than the original. This technique avoids the spectral leakage suffered by forming the filter bank first and then transforming back to the Fourier domain to deconvolve.

By splitting the input signal into subbands, the dispersive smearing that has to be accounted for is essentially reduced to that of an individual subband. This means that to first order the number of samples required for the initial forward transform is inversely proportional to the number of subbands in the filter bank. Consequently, forming such a "coherent filter bank" uses much shorter transforms than single-channel coherent dedispersion. In practical terms this means that the algorithm can use high-speed memory more exclusively and therefore is computationally faster.

Coherent dedispersion and channel summing were repeatedly applied to cover a range of dispersion measures (DMs) typically within ± 0.1 pc cm^{-3} of the published pulsar DM. This guaranteed that our sensitivity would never be reduced due to DM error. Data were square-law detected and combined to give a data set with bandwidth of 64 or 128 MHz. These time series were then searched for broadband emission by summing adjacent samples at time resolutions between 1 and 128 μs. Any two samples with total flux 13 σ (11 σ for PSR J0218+4232) or more above the local mean were further reduced to produce candidate plots for human scrutiny.

Table 1 summarizes the observations taken. Columns (1)–(3) show the pulsar name, center frequency, and bandwidth, respectively. Columns (4) shows the observation duration, and column (5) shows the number of pulses observed. The mean pulse energy and 1 μs sensitivity threshold are shown in columns (6) and (7), respectively. Column (8) shows the number of individual pulses detected. For PSR J0218+4232, this column shows the number of pulses detected in each of the "A" and "B" pulse-phase regions discussed in § 3.1.1 and shown in Figure 1. The system equivalent flux densities for the frequency bands centered at 825–889 and 1373–1437 MHz ranged between 12–14 and 9.1–9.4 Jy, respectively.

3. SEARCH RESULTS

3.1. PSR J0218+4232

3.1.1. Properties of the Pulses

A total of 155 emission events were detected from PSR J0218+ 4232. As these aligned in two distinct pulse-phase windows (see Fig. 1), they are all identified as individual pulses from PSR J0218+4232. Figure 1 also shows the phases of the pulses relative to X-ray profile and the full width half-maximum (FWHM)
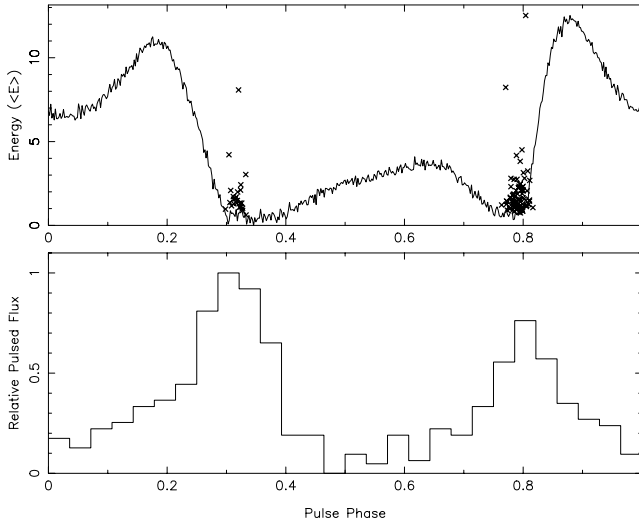
FIG. 1.—*Top*: Phases and energies of pulses detected from PSR J0218+4232 in the 2004 August observation. superimposed on an integrated pulse profile. *Bottom*: The *Chandra* HRC-S 0.08–10 keV pulse profile of PSR J0218+4232 (Kuiper et al. 2004) has been phase-aligned with the radio profile using the absolute timing of Rutledge et al. (2004).

energies of the pulses relative to the mean pulsed flux density. PSR J0218+4232 has a significant ∼50% unpulsed component (Navarro et al. 1995) that was not accounted for in the calculation of the average pulse energy. X-ray emission is more prevalent in the earlier "A" phase window, but more giant pulses were detected at the later "B" phase window. Our observations therefore show that although giant pulses in the radio band appear to orig-

inate in the same part of the pulsar magnetosphere as X-ray emission, they are modulated by different processes. For the August 857 MHz observation, the A and B emission windows spanned 81 μs (0.035 periods) and 123 μs (0.053 periods), respectively. Similar widths of 3% and 4% of phase were measured for the windows at 1373 MHz. The phase regions in which PSR B1937+21 emits giant pulses are much narrower. At 1650 MHz its two windows are 10.7 and 8.2 μs wide, or 0.007 and 0.005 periods wide (Soglasnov et al. 2004). The giant pulses found on the main emission component of PSR J1823−3021A at 685 MHz have a phase range similar to the pulses of PSR J0218+4232, about 0.04 periods or 220 μs (Knight et al. 2005).

The Crab pulsar and PSR B1937+21 emit 10–20 $\langle E \rangle$ pulses at high rates, and so energy thresholds in this range have been used to distinguish giant pulses from ordinary emission (Argyle & Gower 1972; Cognard et al. 1996). Only 3 of the 139 pulses seen at 857 MHz from PSR J0218+4232 had energies greater than 10$\langle E \rangle$, and so this pulse population is not particularly strong compared to the giant pulse populations of the Crab pulsar and PSR B1937+21. However, the argument that these pulses arise from the same giant pulse emission mechanism is compelling. First, the cumulative distribution of pulse energies shown in Figure 2 shows that the strongest pulses have power-law statistics. The tapering off at low energies is caused by the widths of the pulses being underestimated due to noise. The pulses are very narrow and align in phase with the nonthermal X-ray pulses. All these properties are shared by the giant pulses of the Crab pulsar and PSR B1937+21. In addition, the pulses from PSR J0218+4232 occur at the minima of the integrated emission profile and therefore do not contribute to the main emission components. Consequently, they cannot be interpreted as strong
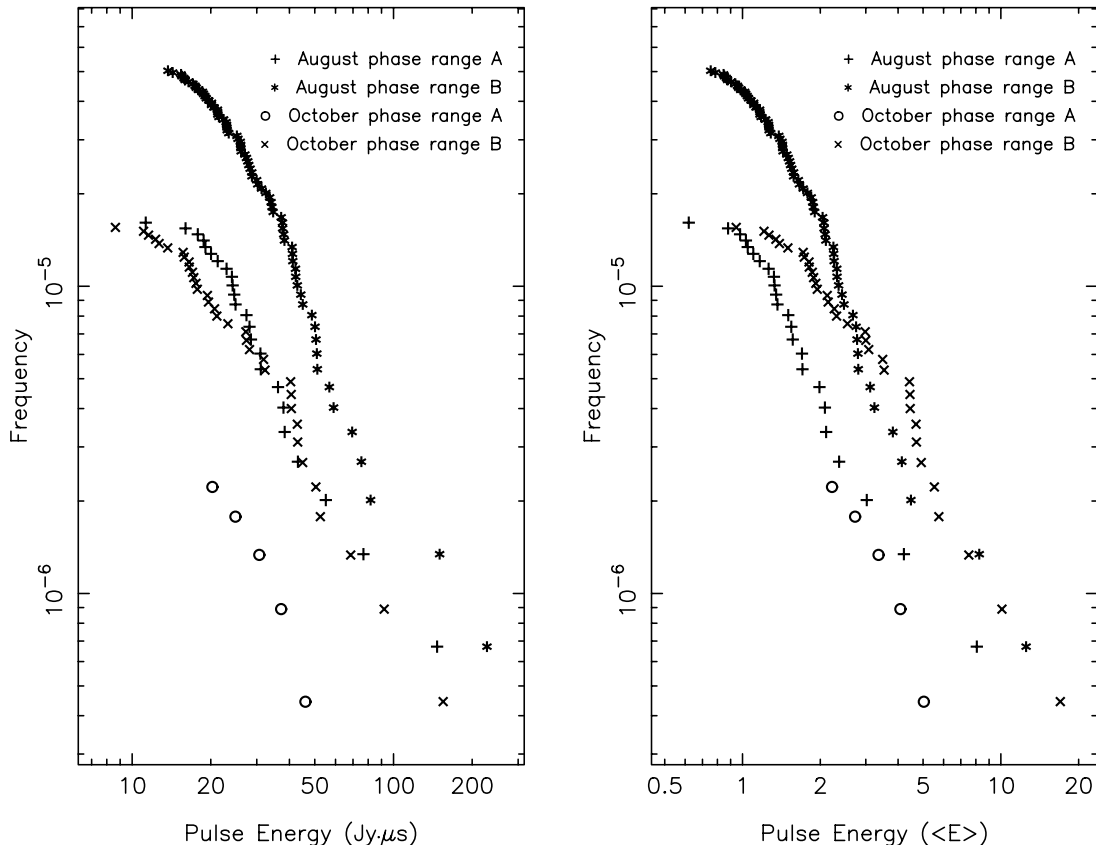

FIG. 2.—Cumulative distribution of giant-pulse energies for observations of PSR J0218+4232 centered at 857 MHz when viewed in terms of absolute energy (*left panel*) and relative to the mean pulse energy (*right panel*).

TABLE 2
Giant-Pulse Emission Rates from a Selection of Pulsars

PSR (1)	ν (MHz) (2)	Phase Range (3)	K (4)	α (5)	$P(E > 20\langle E \rangle)$ (6)	$S_{\mathrm{GP}}(E > 20\langle E \rangle)$ (7)	$S_{\mathrm{GP}}(E > 0.1\langle E \rangle)$ (8)	Reference (9)
J0218+4232....................	857	A (Aug)	1.2×10^{-5}	1.5	1.3×10^{-7}	8.0×10^{-6}	1.1×10^{-4}	This work
J0218+4232....................	857	B (Aug)	5.6×10^{-5}	1.9	1.9×10^{-7}	8.0×10^{-6}	9.4×10^{-4}	This work
J0218+4232....................	857	B (Oct)	4.4×10^{-5}	1.7	2.7×10^{-7}	1.3×10^{-5}	5.4×10^{-4}	This work
J0218+4232....................	1373	all	3.4×10^{-5}	1.5	3.8×10^{-7}	2.3×10^{-5}	3.2×10^{-4}	This work
B1957+20[a]	825	main pulse	2×10^{-5}	2	5×10^{-8}	2×10^{-6}	4×10^{-4}	This work
B0531+21 (Crab)........................	146	main pulse	2.8×10^{-1}	2.5	1.5×10^{-4}	5.1×10^{-3}	n/a	1
B0531+21 (Crab)........................	800	all	9.8	2.4	8.3×10^{-3}	2.9×10^{-1}	n/a	2
B0540−69....................	1390	early	2.4×10^{-2}	1.5	2.7×10^{-4}	1.6×10^{-2}	n/a	3
B0540−69....................	1390	late	7.6×10^{-1}	2.1	1.4×10^{-3}	5.3×10^{-2}	n/a	3
B0540−69....................	1390	all	2.6×10^{-1}	1.8	1.2×10^{-3}	5.4×10^{-2}	n/a	3
B1937+21....................	430	all	3.2×10^{-2}	1.8	1.5×10^{-4}	6.6×10^{-3}	n/a	4
B1937+21....................	1650	all	2.8×10^{-4}	1.4	4.2×10^{-6}	3.0×10^{-4}	2.5×10^{-3}	5

[a] Rates are indicative only due to the very small number of pulses analyzed.

References.—(1) Argyle & Gower 1972; (2) Lundgren et al. 1995; (3) Johnston et al. 2004; (4) Cognard et al. 1996; (5) Soglasnov et al. 2004.

"ordinary" pulses. The pulses from PSR J0218+4232 therefore demonstrate that the giant pulse phenomenon can no longer be defined through arbitrary bounds on pulse energy. Better phenomenological criteria are narrow pulse widths, power-law statistics, and emission occurring in narrow phase windows that align with nonthermal X-ray emission.

Johnston & Romani (2004) also suggested that power-law statistics and emission at special phases were the defining characteristics of giant pulses. Their filter bank observations in previous work (Romani & Johnston 2001) were unable to constrain the width of the giant pulses from PSR B1821−24. Our observations have shown that PSRs J1823−3021A (see Knight et al. 2005) and J0218+4232 have intrinsically narrow pulses. We argue that giant pulses always have narrow widths, and that this property can be added to those presented by Johnston & Romani in defining the giant pulse phenomenon.

The fraction of pulses detected at phase A almost halved, from 0.24 in August to 0.13 in October. As the search did not discriminate on the basis of phase, this difference could be interpreted as being due to variation in the rate of giant pulse emission for each phase window. However, the rate change only becomes readily apparent when viewed in terms of the detection counts regardless of pulsar flux (see left panel of Fig. 2), and not when viewed in terms of energy relative to the mean pulse energy (see right panel of Fig. 2). Small-number statistics are therefore a more likely cause of the disparity: the nondetection of ∼6 low-energy pulses can explain the rate change.

3.1.2. Comparison of Emission Rates

The probability of a pulse having energy greater than E_0 can be expressed as

$$P(E > E_0) = K E_0^{-\alpha}, \qquad (1)$$

where E_0 is in units of the mean pulse energy. Integrating gives an expression for the fraction of pulse flux emitted in the form of giant pulses of energies greater than E_0,

$$S_{\mathrm{GP}}(E > E_0) = \frac{K\alpha}{\alpha - 1} E_0^{1-\alpha}. \qquad (2)$$

The best fits for the 857 MHz pulses with energies greater than 25 Jy μs are shown in Table 2. No satisfactory fit was

obtained for the October A pulses. Estimates of the relative rate at 1373 MHz and rates for other pulsars are also shown. The first three columns show the pulsar, center frequency, and the phase range for which the power law is valid. Columns (4) and (5) show the best fits for K and α. The probability that a pulse has $E > 20\langle E \rangle$ is shown in column (6). Columns (7) and (8) show the fraction of flux that is emitted as giant pulses of energies greater than $20\langle E \rangle$ and $0.1\langle E \rangle$, respectively.

The power-law energy distributions of the Crab pulsar, PSR B0540−69, and PSR B1937+21 (at 430 MHz) do not extend to energies as low as $0.1\langle E \rangle$. Soglasnov et al. (2004) find that at 1650 MHz the giant pulses from PSR B1937+21 extend to energies of 0.016–0.032 $\langle E \rangle$. The power-law exponents for the millisecond pulsars PSR B1821−24 and PSR J1823−3021A are poorly known. However, at 1400–1500 MHz they emit a giant pulse of more than $28\langle E \rangle$ at frequencies of $\sim 8.5 \times 10^{-7}$ and $\sim 4.6 \times 10^{-6}$, respectively (Romani & Johnston 2001; Knight et al. 2005). For comparison, the work of Soglasnov et al. gives for PSR B1937+21 an emission rate of $P(E > 28\langle E \rangle) = 2.6 \times 10^{-6}$. The observed pulse energy distribution is the product of the intrinsic distribution and the spectra of propagation effects such as interstellar scintillation. Scintillation is particularly strong for PSR B1937+21 on timescales of minutes at frequencies in the vicinity of 1–2 GHz and could potentially lead to different studies obtaining different results. Kinkhabwala & Thorsett (2000) obtain parameters for PSR B1937+21 at 1420 MHz of $\alpha = 1.8$ and $P(E > 28\langle E \rangle) \sim 4.0 \times 10^{-7}$, which are quite different from those found by Soglasnov et al.

It is apparent in Table 2 that PSR J0218+4232 has a much lower rate of giant pulse emission than other giant pulse emitters. The total fraction of its pulsed energy emitted in the form of giant pulses with energies greater than $0.1\langle E \rangle$ is about 0.1%. Such giant pulses can occur at rates of up to 1 per ∼200 pulsar rotations. If the cutoff point of the power law occurs at $0.1\langle E \rangle$, then the ∼10% of the pulse profile where the giants occur should have a flux enhancement caused by the giant pulses of ∼1% of the mean flux density. If the power law extends to $0.01\langle E \rangle$, then the flux enhancement increases to the 10% level. Extension to energies much lower than $0.01\langle E \rangle$ does not seem plausible given the lack of large components in the emission regions of the giant pulses.

The power-law fit for the 10 most energetic pulses seen at 1373 MHz is summarized in Table 2. A $20\langle E \rangle$ pulse at 1373 MHz is emitted about 1.7 times more frequently than the August
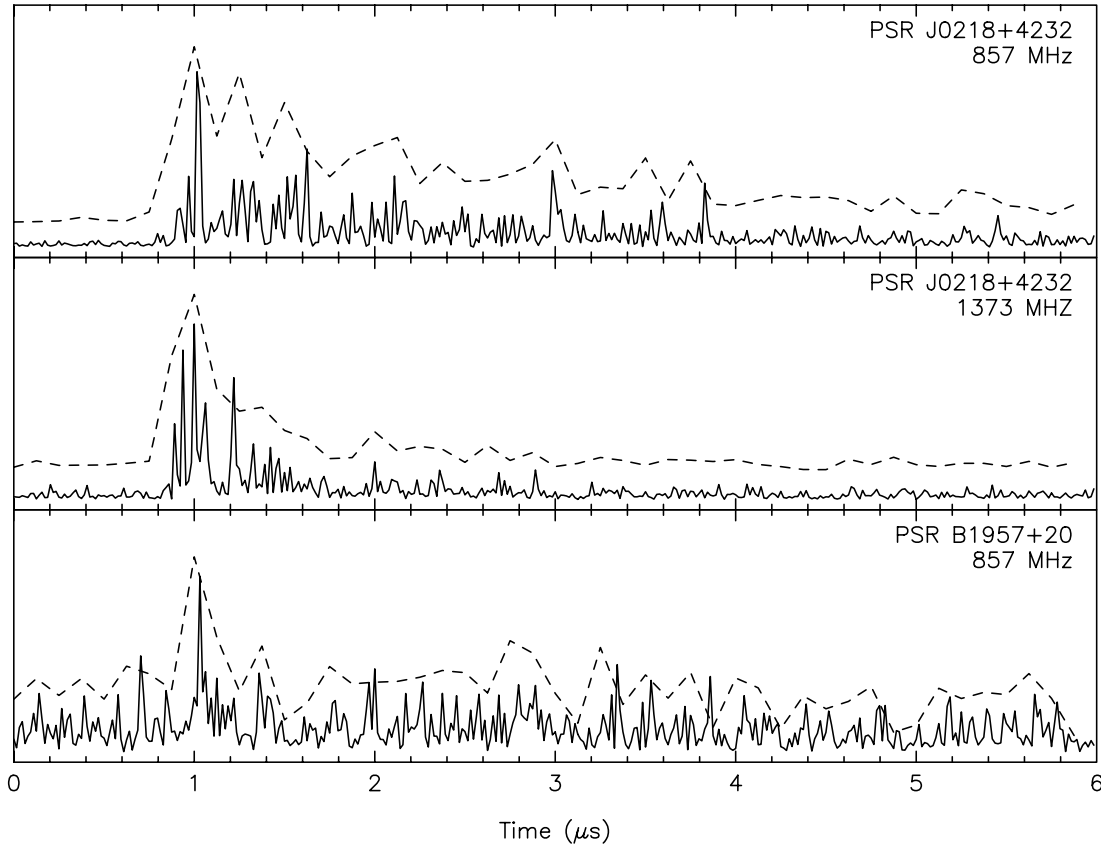
Fig. 3.—Intensity of the central portion of the strongest giant pulses from PSR J0218+4232 and PSR B1957+20 when seen with a sampling interval of 15.625 ns (*solid line*) and 125 ns (*dashed line*).

857 MHz B pulses. It should be noted that the formal uncertainty on α of ± 0.1 makes this estimate somewhat uncertain.

3.1.3. *Pulse Durations*

All the 857 MHz pulses had FWHM durations of ≤ 3.2 μs. The strongest pulse had a FWHM duration of 2.6 μs. To investigate the possibility of substructure, this pulse was coherently dedispersed at a time resolution of 15.625 ns. The initial portion of the pulse is shown in the top panel of Figure 3. The finite rise time is only resolved at sampling intervals less than 125 ns and persists if the DM is slightly altered. At high time resolution the noise statistics are better modeled using χ^2 distributions than with the standard Gaussian approximation. The noise statistics therefore become more positively skewed at higher time resolutions, and so much of the substructure seen at 15.625 ns time resolution is likely to be spurious.

The strongest pulse seen at 1373 MHz, as shown in the middle panel of Figure 3, is significantly narrower. At a time resolution of 125 ns it is of order 500 ns wide.

Strong spikes following the main emission peak persist for about 8 times longer at 857 MHz than at 1373 MHz, and so the pulse widths are roughly consistent with the $\nu^{-4.4}$ scaling law of Kolmogorov spectrum interstellar scattering (Bhat et al. 2003). We think the finite rise time seen at both 857 and 1373 MHz is a consequence of propagation through a thick scattering screen (see, e.g., Williamson 1973) rather than intrinsic substructure.

3.1.4. *Timing of Giant Pulses*

The giant pulse emission of PSR J0218+4232 occurs over much narrower ranges of pulse phase than the integrated pulses. It is therefore important to consider whether timing of PSR J0218+4232 can be improved by timing only the giant pulses. We formed a standard profile from the brightest giant pulse and cross-correlated the giant pulses with it to obtain an arrival time. The 56 giant pulses in the August observation in phase range B that had arrival time errors less than 0.5 μs had an rms residual of 24 μs. The error in arrival time for the whole group was therefore about 3 μs. However, our timing of the mean profile for this observation obtains an rms residual of 6 μs using 16.8 s integrations, which we would expect to improve significantly with increased integration. Therefore, conventional timing gives superior results to timing using giant pulses.

3.2. *PSR J1012+5307*

PSR J1012+5307 is a 5.3 ms pulsar with a characteristic age of 8.6 Gyr (Lange et al. 2001). It has a B_{LC} 68 times smaller than that of PSR B1937+21. No individual pulses were detected from PSR J1012+5307. Our result is consistent with the fact that to date no millisecond pulsars with low values of B_{LC} and large characteristic ages have been observed to emit giant pulses. Edwards & Stappers (2003) observed PSR J1012+5307 for 1800 s at 1380 MHz using the Westerbork Synthesis Radio Telescope. With a sampling interval of 51.2 μs, they detected 70 individual pulses with energies of up to 5 times the mean pulse energy. Our observations establish that it is very unlikely that the pulses uncovered by Edwards & Stappers have the short $\lesssim 1$ μs timescales characteristic of the giant pulses of PSR B1937+21.

3.3. *PSR B1957+20*

PSR B1957+20 has the third highest B_{LC} of all millisecond pulsars and was therefore targeted by Knight et al. (2005) as a potential source of giant pulse emission. Knight et al. failed to
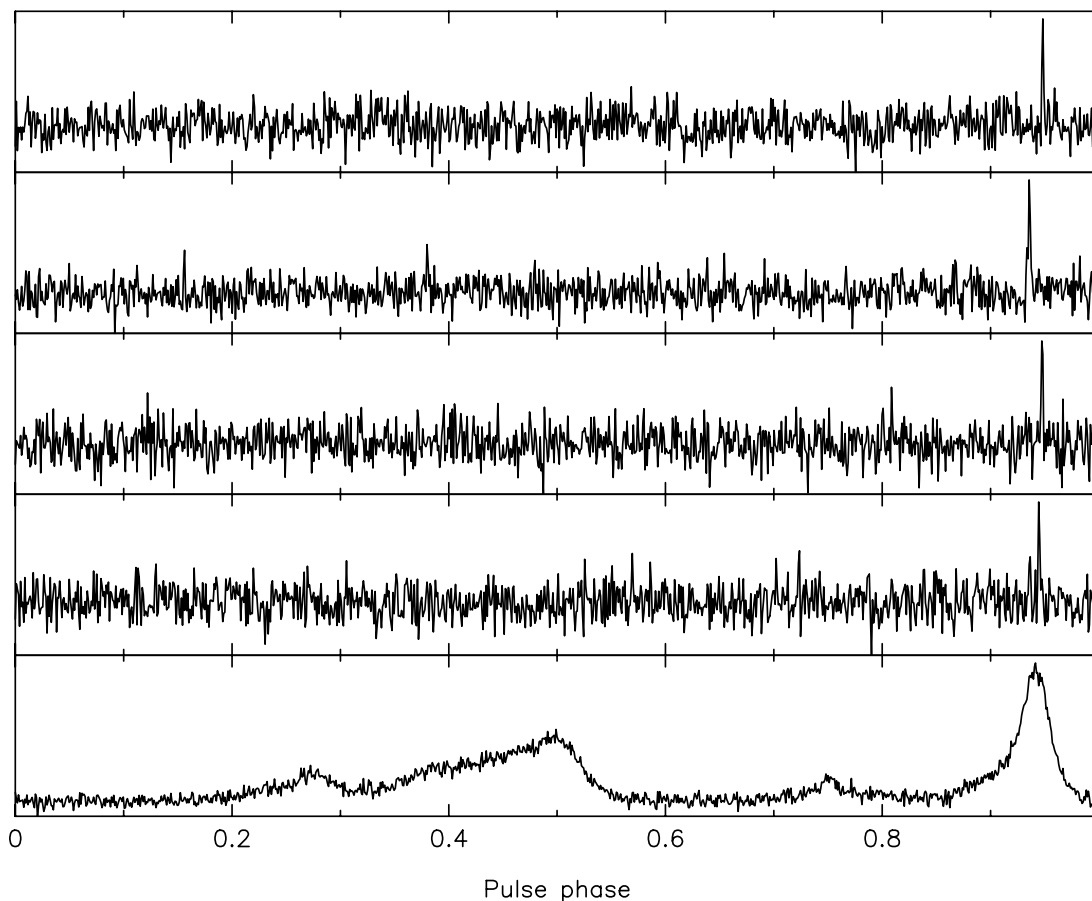
Fig. 4.—Relative phases of the individual pulses detected from PSR B1957+20. The top four panels show the intensities of the pulses, and the bottom panel shows the intensity of the integrated pulse profile.

detect any pulses in 7700 s of observations at a center frequency of 685 MHz using the Parkes Radio Telescope. It is well known that the pulsar wind of PSR B1957+20 causes gas to be ablated from its companion (Fruchter et al. 1990; Krolik & Sincell 1990). This ionized gas causes eclipses at orbital phases (ϕ) near 0.25. Knight et al. had suggested that the gas could scatter-broaden any giant pulses beyond reasonable detection levels. How-ever, significant broadening cannot occur at all orbital phases, as in 8003 s of observations using the GBT we detected four narrow pulses from PSR B1957+20. Our observations spanned $0.40 < \phi < 0.67$; the earliest pulse arrived at $\phi = 0.41$.

To estimate the energies of the pulses, we formed a 512 bin profile of each pulse and calculated the FWHM energy. The pulses had energies of 4.5–8.6 $\langle E \rangle$. At this coarse time resolution vir-tually all of the pulse flux for these pulses is encompassed in our estimate. Adjustment of the DM used for coherent dedispersion and channel summing causes changes in the noise characteristics of the on-pulse region. Peak intensity, pulse morphology, and pulse width all vary with DM, and so determination of the true DM and therefore true pulse shape becomes dependent on the exact criteria used to optimize DM. The bottom panel of Figure 3 shows the strongest pulse. Although the main pulse component appears very narrow, there is a very weak underlying emission region about it, of microsecond duration. Other pulses optimize at DMs that differ by $O(10^{-3})$ pc cm^{-3}. We think that this DM uncertainty is caused by the low signal strength of the pulses. It means that the profiles shown at high time resolution do not necessarily represent the true pulse form. For weak pulses like these, we suggest that the true nature of the pulses in terms of their

individual DMs, intrinsic widths, and substructure requires the DM to be accurately determined via multifrequency observations.

The four pulses fall in a narrow 20 μs pulse window that covers the peak of the main emission component (see Fig. 4). The other pulse components of the integrated profile are 50% or more weaker than the main component. It is reasonable to suppose that PSR B1957+20 might emit narrow pulses similar to those observed that are phase-aligned with the other components. If these pulses exist and are amplitude modulated in a similar fashion to the "ordinary" pulse emission, they would be 50% or more weaker than the main-component pulses we see. As our initial detection threshold was 13 σ and the main-component pulses were detected at 14–16 σ, our ob-servations do not place good bounds on the existence of such pulses.

3.4. PSR J1843−1113

PSR J1843−1113 is a solitary 1.8 ms pulsar with a characteristic age of ∼3 Gyr. Its B_{LC} is very high—about 0.2 times that of PSR B1937+21. No spikes of broadband emission were detected from it, suggesting that if it does emit giant pulses, they are very weak and/or infrequent. Because PSR J1843−1113 is close to the plane of the Galaxy and has a relatively high DM, we cannot rule out the possibility that it emits pulses similar to those of PSR B1957+20, but that are scatter-broadened beyond our sensitivity limits.

4. DISCUSSION

4.1. Pulse Populations

Joshi et al. (2004) reported the detection of an unresolved ∼129$\langle E \rangle$ (925 Jy μs) large-amplitude pulse from PSR B1957+20

in observations centered at 610 MHz. As this pulse is much larger than any detected in our observations, it is instructive to consider whether it constitutes: (1) a member of a different pulse population of longer intrinsic duration; (2) the very high energy tail of the distribution we observed; or (3) some sort of noise event that is unrelated to the pulsar. If the pulse reported by Joshi et al. is as broad as their sampling time (258 μs), then our 825 MHz detection threshold for summing two 128 μs samples of $45\langle E \rangle$ should have found similar pulses, and so our observations are not consistent with hypothesis (1). Alternatively, if we assume the pulses follow a $\alpha = -1.4$ energy distribution, then our observations imply that a $129\langle E \rangle$ pulse should be emitted on average once every 61 hr. Given that Joshi et al. observed PSR B1957+20 for ≤ 1 hr and that much steeper power-law distributions have been found for other giant pulse emitters (see, e.g., Romani & Johnston 2001), we find hypothesis (2) untenable. The detection criterion used by Joshi et al. was that a pulse must exceed 3.5 σ in two bands. With an rms of ~ 1 Jy over their 16 MHz band, it is apparent that a bare detection corresponds to 1300 Jy μs, or $180\langle E \rangle$. For a normally distributed noise floor, approximately 11 noise spikes would be expected to exceed this threshold in their sample of $\sim 10^6$ pulses. The fact that multiple noise spikes with higher energies than the pulse are expected to be present in the Joshi et al. data makes it difficult to argue that the pulse is not background noise. This in turn implies that we have presented the first evidence for a population of giant pulses from PSR B1957+20.

Joshi et al. (2004) also reported the detection at 610 MHz of three unresolved large-amplitude ~ 258 μs wide pulses from PSR J0218+4232 with energies of 48–51 $\langle E \rangle$. The event rate of this pulse population is $P(E > 48\langle E \rangle) = 1.4 \times 10^{-6}$, which is 40 times higher than our August rate for the B phase range of $P(E > 48\langle E \rangle) = 3.6 \times 10^{-8}$. Our August detection threshold for summing two 128 μs samples of $7\langle E \rangle$ means that we should have easily detected the Joshi et al. pulses. Therefore, the pulses of Joshi et al. are not a separate pulse population that is simply stronger than the one we observed. Furthermore, the Joshi et al. pulses occur at a different phase than the pulses we saw, so the hypothesis that Joshi et al. were extremely fortunate in detecting the high-energy tail of our population is not at all plausible. Pulses similar to those reported by Joshi et al. should also have been seen by Edwards & Stappers (2003), who did not detect any pulses above $26\langle E \rangle$ in an 1800 s observation centered at 328 MHz. If the noise floor of Joshi et al. is normally distributed, then approximately 36 noise spikes in their sample would be expected to exceed their criterion of 3.5 σ in both bands and therefore have an energy similar to that of the pulses reported. The three pulses are therefore not distinguishable from background noise and are likely to be spurious. The only type of strong pulses not ruled out by our data reduction are those with timescales comparable to PSR J0218+4232's 2.3 ms pulse period. However, such pulses probably would have had substructure detectable in our searches. It is more likely that PSR J0218+4232 only emits one population of strong pulses, the population of giant pulses unveiled by our observations.

4.2. Giant Pulses from PSR B1957+20

The pulses seen from PSR B1957+20 have submicrosecond timescales and are several times stronger than the mean pulse. All four coincide with the main emission component in a fashion similar to the giant pulses of PSR J1823−3021A. Even without evidence for power-law statistics, it is tempting to categorize PSR B1957+20 as a giant pulse emitter. However, the pulses can also be explained as strong pulses of ordinary emission that are ex-

ceptionally narrow. This hypothesis is supported by the fact that pulses from PSR J0437−4715 exhibit an anticorrelation between pulse width and pulse strength (Jenet et al. 1998). The strongest "ordinary" pulses from PSR J0437−4715 are then much more readily detected in single-pulse searches, and therefore could potentially masquerade as a giant-like population. Jenet et al. found pulses as short as 10 μs in their ~ 3000 s of observations. Therefore it is not unreasonable to suggest that in ~ 8000 s PSR B1957+20 could emit several ordinary pulses consisting of very short spikes superimposed on microsecond-timescale emission bursts. The fact that we did not detect any microsecond-timescale emission from PSR J1012+5307 means the pulse substructure seen by Edwards & Stappers (2003) is broader than that seen for PSR B1957+20. Similarly, Knight et al. (2005) did not find any substructure in pulses from PSR J1603−7202 as short as their 4 μs sampling time. Microstructure within ordinary pulses from millisecond pulsars therefore does not seem to have characteristic timescales as short as those of the PSR B1957+20 pulses.

Insight into whether or not the pulses from PSR B1957+20 are plausibly "giant" can be gained by comparing the properties of PSR B1957+20 and pulsars that emit giant pulses. Table 3 summarizes the attributes of the millisecond pulsars previously known to emit giant pulses (top three rows) and the pulsars we observed (bottom four rows). Each of these two groups is sorted by right ascension. The first three columns show the pulsar name, period, and period derivative, respectively. The period derivatives have been corrected for kinematic effects where possible (Shklovskii 1970; Damour & Taylor 1991). PSRs B1821−24 and J1823−3021A are located within globular clusters, and so acceleration in the cluster potential will contribute to the observed $\dot{P}$ for these pulsars. The magnitude of the cluster contribution to $\dot{P}$ is very uncertain, but has been estimated to be $\leq 0.06\dot{P}$ for PSR B1821−24 (Phinney 1993) and $\leq 0.7\dot{P}$ for PSR J1823−3021A (Stappers 1997). The proper motions of PSRs J0218+4232 and J1843−1113 are unknown, but a 100 km s^{-1} velocity equates to a Shklovskii-term contribution to $\dot{P}$ of just 0.6% for PSR J0218+4232 and 10% for PSR J1843−1113. Columns (4)–(7) of Table 3 show derived quantities: the characteristic age, the magnetic field at the light cylinder, the spin-down luminosity, and the complexity parameter $[a_c \approx 5(\dot{P}/10^{-15})^{2/7}P^{-9/14}]$ as presented by Gil & Sendyk (2000) and discussed by Gil & Melikidze (2005). Column (8) gives spectral indices (α_{spec}), and column (9) summarizes the X-ray luminosities of the pulsars. These are given for the 2–10 keV band unless otherwise stated.

PSR B1957+20 has comparable values of B_{LC}, $\dot{E}$, and a_c to the four millisecond pulsars that emit giant pulses. Young pulsars like PSR B0540−69 and the Crab have much higher values of $\dot{E}$ and a_c, but they also emit many more giant pulses. If any of these attributes dictate giant pulse emissivity, we would expect PSR B1957+20 to emit giant pulses. If the pulses we see are not giant pulses, then it is plausible that there is another population of pulses that has an even lower rate of emission. Presumably these pulses would take the form of very narrow spikes that are restricted in pulse phase, just like the pulses we see. As invoking two populations of identical looking pulses is contrived, we believe that we have seen purely giant pulse emission, or giant pulse emission superimposed on a base of ordinary emission. An alternate idea, which we do not favor, is that at moderate energies ordinary and giant pulses are indistinguishable because the two seemingly disparate populations share a common emission mechanism. The ordinary pulses of PSR B1937+21 show no sign of modulation (Jenet & Gil 2004), and the giant pulses only marginally coincide with the envelope of ordinary emission. The emission mechanisms are therefore quite distinct for PSR B1937+21, and consequently

PSR (1)	P (ms) (2)	$\dot{P}$ ($\times 10^{-21}$) (3)	τ (Myr) (4)	B_{LC} (10^4 G) (5)	$\dot{E}$ (10^{33} ergs s^{-1}) (6)	a_c (7)	α_{spec} (8)	$L_{X(2-10\ keV)}$ (10^{32} ergs s^{-1}) (9)	References (10)
Previously Known Giant Pulse Emitters									
J1823−3021A[a]	5.44	3390	26	25	810	28	−2.7	unknown	1, 2
B1821−24[a]	3.05	1620	30	74	2200	33	−2.3	13, 12.8 (0.5−8 keV)	1, 3, 4, 5
B1937+21	1.56	106	230	102	1100	23	−2.6	0.5−5.7	1, 3, 6, 7, 8
Observed Pulsars									
J0218+4232	2.32	77.4	480	32	240	16	−3.0	1.3 (1−10 keV); 1.2−1.6	1, 9, 10, 11, 12
J1012+5307	5.26	9.73	8600	1.5	2.6	6.3	−1.9	0.003 (0.2−10 keV)	13, 14, 15
J1843−1113	1.85	9.59	3100	20	59	11	unknown	unknown	1
B1957+20	1.61	11.5	2200	31	110	14	−3.0	0.16 (0.5−7 keV)	1, 6, 16, 17

[a] Parameters ignore acceleration in the gravitational potential of the host cluster.

REFERENCES.—(1) Manchester et al. 2005; (2) Toscano et al. 1998; (3) Foster et al. 1991; (4) Becker et al. 2003; (5) Mineo et al. 2004; (6) Toscano et al. 1999; (7) Takahashi et al. 2001; (8) Nicastro et al. 2004; (9) Navarro et al. 1995; (10) Mineo et al. 2000; (11) Kuiper et al. 2002; (12) Webb et al. 2004a; (13) Nicastro et al. 1995; (14) Lange et al. 2001; (15) Webb et al. 2004b; (16) Fruchter et al. 1990; (17) Stappers et al. 2003.

it seems unlikely that the population of pulses from PSR B1957+20 represents the transition of a single pulse population from ordinary-like to giant-like emission. At this stage we cannot definitely state that PSR B1957+20 emits giant pulses. Further supporting evidence could be made by establishing power-law statistics and finding a correlation in phase with an X-ray pulse. The general task of identifying weak pulses as giant pulses is more difficult. Evidence could include giant pulses having different DMs to ordinary pulses, or characteristic timescales much shorter than those seen for microstructure.

Although PSR B1957+20 has a B_{LC} similar to that of the millisecond pulsars that emit giant pulses, its emission rate is significantly lower. In particular, its rate would appear to be ∼100 times lower than PSR B1823−3021A, despite the fact that PSR B1957+20 has a higher B_{LC}. Magnetic inclination angle and other geometric factors must play some role, but it is difficult to see how they could account for such an enormous difference in emissivity. So although the magnetic field at the light cylinder does seem to be a reasonable determinant of whether or not a pulsar emits giant pulses, alone it is not a trustworthy indicator of the rate of emissivity.

4.3. Giant Pulse Emitters

PSR J0218+4232 is the fourth millisecond pulsar found that has been shown conclusively to emit giant pulses. All four such millisecond pulsars have high values of $\dot{E}$ and the complexity parameter. The three observed in X-rays are very luminous in the 2−10 keV band and have hard photon indices (see Table 3 and references therein). It is tempting to suggest that one or more of these characteristics are better indicators of emissivity rates than B_{LC}. However, PSRs B1957+20 and J1843−1113 do not have corresponding values that are so much lower that $\dot{E}$, and the complexity parameter can be discriminated from B_{LC} as the primary determinant of whether or not a millisecond pulsar emits giant pulses. In fact, B_{LC}, $\dot{E}$, and the complexity parameter have such similar P-$\dot{P}$ dependences that we do not think observations of millisecond pulsars can ever discriminate between them.

Which other millisecond pulsars could emit giant pulses? Pulsars with high B_{LC} still seem to be good candidates, but this parameter no longer appears to guarantee a rate sufficiently large to give a high detection count. Table 3 shows that the millisecond pulsars that emit giant pulses all have spectral indices much

steeper than the $\alpha_{spec} = -1.9$ average of the millisecond pulsars observed by Toscano et al. (1998). They also have very low characteristic ages and high X-ray luminosities. Perhaps better sources are young or X-ray luminous pulsars in globular clusters? Unfortunately, the Galactic globular cluster population is old and so most cluster pulsars are likely to be too old to be good candidates for giant pulse emission. Consider PSR J0024−7204J, which has a 0.5−6 keV X-ray flux of $L_X = 2 \times 10^{31}$ ergs s^{-1} (Heinke et al. 2005). This is a luminosity similar to that of PSR B1957+20, so we do not expect PSR J0024−7204J to emit giant pulses at a high rate. Since PSR J0024−7204J has the highest X-ray luminosity of the identified millisecond pulsars in 47 Tucanae, we do not consider 47 Tucanae to be a good candidate cluster for giant pulse emission. The clusters most likely to host populations of the young and X-ray luminous millisecond pulsars prone to emitting giant pulses are instead those that appear to contain young pulsars, such as the core-collapsed clusters M15 and NGC 6624.

Perhaps all millisecond pulsars emit giant pulses at even lower rates than PSR B1957+20? The best candidates for verifying this hypothesis are nearby millisecond pulsars that have pulses that are not significantly scatter-broadened. Should bright pulsars like PSR J0437−4715 emit nanosecond-timescale pulses, then high time resolution studies could potentially probe their pulse populations down to very low energies. Such studies could reveal giant pulses occurring at rates smaller by factors of ∼1000 than seen for PSR B1957+20.

5. CONCLUSIONS

We have searched four millisecond pulsars for individual pulses of emission with microsecond timescales and have found such emission from two of them. Only four individual pulses were detected from PSR B1957+20 in 8003 s of observations centered at 825 MHz. As these pulses are exceptionally narrow, there is little scattering-induced pulse broadening at at least some orbital phases. Although it is debatable whether or not these strong pulses are true "giant pulses," we can say that the giant pulse emission rate from PSR B1957+20 is significantly less than the rates for other pulsars with similar values of magnetic field at the light cylinder. Although B_{LC} can be used as a rough guide to whether a pulsar emits giant pulses, we suggest that it is a poor indicator of the emission rate.

PSR J0218+4232 emits giant pulses at a low rate that is inconsistent with the findings of Joshi et al. (2004). It is most likely that the pulses reported by Joshi et al. are spurious. The giant pulses of PSR J0218+4232 are confined to two narrow phase regions separated by roughly 50% of phase, which align in phase with the peaks of the X-ray profile and roughly coincide with the minima of the integrated pulse profile in the radio band. This strong correlation between X-ray and radio properties confirms that the two emission processes originate in similarly defined regions of the pulsar magnetosphere.

Most of the 139 giant pulses observed from PSR J0218+4232 at a center frequency of 857 MHz had relatively low energies, typically only a few times the mean pulse energy. Only three had energies above $10\langle E \rangle$, and none had energies above $20\langle E \rangle$. The pulses exhibit power-law statistics, are only found in narrow phase windows that coincide in phase with the X-ray pulse components, and are very narrow, just like the giant pulses of PSR B1937+21; it is apparent then that "giant" pulses should be defined not through large flux densities, but by these three properties. The brightest pulse seen at a center frequency of 1373 MHz seems to be around 500 ns in duration when viewed at 125 ns time resolution. At higher time resolution, finer features become apparent, but it is unclear whether these are significant.

PSR J0218+4232 is the fourth millisecond pulsar found to emit giant pulses, after PSRs B1937+21, B1821−24, and J1823−3021A. All four have low characteristic ages and steep radio spectra. With the exception of PSR J1823−3021A, which has not been observed in X-rays, the four pulsars all have high X-ray luminosities and exhibit power-law spectra. The presence of X-ray emission with a steep power-law spectrum therefore seems to be the best indicator of whether a millisecond pulsar emits giant pulses. Radio observations would be expected to show that narrow giants will be present at the phase of the X-ray emission.

REFERENCES

Argyle, E., & Gower, J. F. R. 1972, ApJ, 175, L89
Becker, W., & Trümper, J. 1999, A&A, 341, 803
Becker, W., et al. 2003, ApJ, 594, 798
Bhat, N. D. R., Cordes, J. M., & Chatterjee, S. 2003, ApJ, 584, 782
Cairns, I. H., Johnston, S., & Das, P. 2004, MNRAS, 353, 270
Cognard, I., Shrauner, J. A., Taylor, J. H., & Thorsett, S. E. 1996, ApJ, 457, L81
Cordes, J. M. 1976, ApJ, 210, 780
Cordes, J. M., Bhat, N. D. R., Hankins, T. H., McLaughlin, M. A., & Kern, J. 2004, ApJ, 612, 375
Cusumano, G. 2004, Adv. Space Res., 33, 495
Cusumano, G., Hermsen, W., Kramer, M., Kuiper, L., Löhmer, O., Massaro, E., Mineo, T., Nicastro, L., & Stappers, B. W. 2003, A&A, 410, L9
Damour, T., & Taylor, J. H. 1991, ApJ, 366, 501
Edwards, R. T., & Stappers, B. W. 2003, A&A, 407, 273
Foster, R. S., Fairhead, L., & Backer, D. C. 1991, ApJ, 378, 687
Fruchter, A. S., et al. 1990, ApJ, 351, 642
Gil, J. A., & Melikidze, G. I. 2005, A&A, 432, 61
Gil, J. A., & Sendyk, M. 2000, ApJ, 541, 351
Grindlay, J. E., Camilo, F., Heinke, C. O., Edmonds, P. D., Cohn, H., & Lugger, P. 2002, ApJ, 581, 470
Hankins, T. H., Kern, J. S., Weatherall, J. C., & Eilek, J. A. 2003, Nature, 422, 141
Hankins, T. H., & Rickett, B. J. 1975, in Methods in Computational Physics Vol. 14: Radio Astronomy (New York: Academic Press), 55
Heinke, C. O., Grindlay, J. E., Edmonds, P. D., Cohn, H. N., Lugger, P. M., Camilo, F., Bogdanov, S., & Freire, P. C. 2005, ApJ, 625, 796
Jacoby, B. A. 2005, Ph.D. thesis, California Inst. Technology
Jenet, F., Anderson, S., Kaspi, V., Prince, T., & Unwin, S. 1998, ApJ, 498, 365
Jenet, F. A., & Gil, J. 2004, ApJ, 602, L89
Johnston, S., & Romani, R. W. 2002, MNRAS, 332, 109
———. 2003, ApJ, 590, L95
———. 2004, in IAU Symp. 218, Young Neutron Stars and Their Environments, ed. F. Camilo & B. M. Gaensler (San Francisco: ASP), 315
Johnston, S., Romani, R. W., Marshall, F. E., & Zhang, W. 2004, MNRAS, 355, 31
Johnston, S., van Straten, W., Kramer, M., & Bailes, M. 2001, ApJ, 549, L101
Joshi, B. C., Kramer, M., Lyne, A. G., McLaughlin, M. A., & Stairs, I. H. 2004, in IAU Symp. 218, Young Neutron Stars and Their Environments, ed. F. Camilo & B. M. Gaensler (San Francisco: ASP), 319
Kinkhabwala, A., & Thorsett, S. E. 2000, ApJ, 535, 365

Knight, H. S., Bailes, M., Manchester, R. N., & Ord, S. M. 2005, ApJ, 625, 951
Krolik, J. H., & Sincell, M. W. 1990, ApJ, 357, 208
Kuiper, L., Hermsen, W., & Stappers, B. 2004, Adv. Space Res., 33, 507
Kuiper, L., Hermsen, W., Verbunt, F., Ord, S. M., Stairs, I. H., & Lyne, A. G. 2002, ApJ, 577, 917
Lange, C., Camilo, F., Wex, N., Kramer, M., Backer, D., Lyne, A., & Doroshenko, O. 2001, MNRAS, 326, 274
Lundgren, S. C., Cordes, J. M., Ulmer, M., Matz, S. M., Lomatch, S., Foster, R. S., & Hankins, T. 1995, ApJ, 453, 433
Manchester, R. N., Hobbs, G. B., Teoh, A., & Hobbs, M. 2005, AJ, 129, 1993
Mineo, T., Cusumano, G., Massaro, E., Becker, W., & Nicastro, L. 2004, A&A, 423, 1045
Mineo, T., et al. 2000, A&A, 355, 1053
Navarro, J., de Bruyn, G., Frail, D., Kulkarni, S. R., & Lyne, A. G. 1995, ApJ, 455, L55
Nicastro, L., Cusumano, G., Löhmer, O., Kramer, M., Kuiper, L., Hermsen, W., Mineo, T., & Becker, W. 2004, A&A, 413, 1065
Nicastro, L., Lyne, A. G., Lorimer, D. R., Harrison, P. A., Bailes, M., & Skidmore, B. D. 1995, MNRAS, 273, L68
Phinney, E. S. 1993, in ASP Conf. Ser. 50, Structure and Dynamics of Globular Clusters, ed. S. G. Djorgovski & G. Meylan (San Francisco: ASP), 141
Romani, R., & Johnston, S. 2001, ApJ, 557, L93
Rutledge, R. E., Fox, D. W., Kulkarni, S. R., Jacoby, B. A., Cognard, I., Backer, D. C., & Murray, S. S. 2004, ApJ, 613, 522
Shklovskii, I. S. 1970, Soviet Astron., 13, 562
Soglasnov, V. A., Popov, M. V., Bartel, N., Cannon, W., Novikov, A. Y., Kondratiev, V. I., & Altunin, V. I. 2004, ApJ, 616, 439
Staelin, D. H., & Reifenstein, E. C., III. 1968, Science, 162, 1481
Stairs, I. H. 1998, Ph.D. thesis, Princeton Univ.
Stappers, B. W. 1997, Ph.D. thesis, Australian National Univ.
Stappers, B. W., Gaensler, B. M., Kaspi, V. M., van der Klis, M., & Lewin, W. H. G. 2003, Science, 299, 1372
Takahashi, M., et al. 2001, ApJ, 554, 316
Toscano, M., Bailes, M., Manchester, R., & Sandhu, J. 1998, ApJ, 506, 863
Toscano, M., Sandhu, J. S., Bailes, M., Manchester, R. N., Britton, M. C., Kulkarni, S. R., Anderson, S. B., & Stappers, B. W. 1999, MNRAS, 307, 925
van Straten, W. 2003, Ph.D. thesis, Swinburne Univ. Technology
Webb, N. A., Olive, J.-F., & Barret, D. 2004a, A&A, 417, 181
Webb, N. A., Olive, J.-F., Barret, D., Kramer, M., Cognard, I., & Löhmer, O. 2004b, A&A, 419, 269
Williamson, I. P. 1973, MNRAS, 163, 345